PLASMA DYNAMICS

XI. PLASMA PHYSICS*

Academic and Research Staff

Prof. G. Bekefi
Prof. S. C. Brown
Prof. J. C. Ingraham
Prof. B. L. Wright
Dr. W. M. Manheimer
J. J. McCarthy
W. J. Mulligan
B. Rama Rao (Visiting Scientist)

Graduate Students

R. J. Becker
A. J. Cohen
D. L. Flannery
L. P. Mix, Jr.
L. D. Pleasance
G. L. Rogoff
J. K. Silk
E. N. Spithas
D. W. Swain
J. H. Vellenga
D. L. Workman

A. ELECTRON MOBILITY, COLLISION FREQUENCY, AND MEAN-FREE PATH IN ARGON

When the cross section for collisions of electrons with gas atoms exhibits a complicated dependence on electron energy, the calculation of various collisional parameters may be difficult. This is the case for nonmonoenergetic low-energy electrons in Argon, because of the Ramsauer minimum in the cross section at an electron energy of approximately 0.3 eV. The difficulty of obtaining an analytic representation for the cross section makes the determination of average collisional quantities (such as average collision frequency or mean-free path) quite difficult. Often these quantities are calculated by using the cross section at some supposedly representative energy, with the resulting deviation from the true averages being somewhat in doubt.

The average mobility, frequency of collision for momentum transfer, and mean-free path for electrons with a Maxwellian electron energy distribution in Argon have been computed as a function of electron temperature by numerical integration. This report presents the results of these calculations, together with comparisons of these results with estimates based on a crude approximation to the collision cross-section dependence on electron energy. Also presented are simple relations between the collisional parameters and electron temperature which closely approximate the numerically computed values.

Figure XI-1 gives the probability of collision for momentum transfer (P_m:cm^{-1}) for electrons in Argon as a function of electron energy (u:eV). This is a smooth curve drawn through the unstarred values listed in Table XI-1. The unstarred values at 30.0 eV and below are derived from the values of the momentum transfer cross section listed by Frost and Phelps[1]; those at 36.0 eV and above result from scaling down the high-energy values[2] of P_c to fit onto the data of Frost and Phelps. The question of the validity of this scaling procedure is unimportant here, since these values have only a

*This work was supported by the U.S. Atomic Energy Commission (Contract AT(30-1)-1842).

Table XI-1. Probability of collision for momentum transfer, P_m (cm^{-1}), as a function of electron energy, u (eV).

u	P_m	u	P_m
0	28.46	1.5	6.15
0.01	21.57	* 1.75	7.5
0.02	13.22	2.0	8.77
0.03	9.9	* 2.5	11.6
0.04	8.1	3.0	14.4
0.05	6.51	* 3.5	17.5
0.07	4.03	4.0	20.5
0.09	1.98	* 5.0	25.7
0.11	1.21	6.0	30.76
0.14	0.831	* 7.0	36.2
0.17	0.693	8.0	41.37
0.2	0.626	* 9.0	45.0
0.25	0.552	10.0	48.79
0.32	0.534	* 11.0	50.0
* 0.36	0.59	12.0	51.26
0.4	0.644	15.0	46.67
* 0.45	0.812	20.0	36.77
0.5	1.0	26.0	29.34
* 0.58	1.33	30.0	25.46
0.65	1.66	36.0	21.0
* 0.74	2.1	44.7	18.0
0.8	2.4	49.0	17.04
* 0.9	3.05	64.0	14.93
1.0	3.71	81.0	13.67
* 1.25	4.9	100.0	12.84

*Value of P_m is obtained from Fig. XI-1 by linear interpolation.

Note: Values of P_m for $u \leq 30.0$ eV from Frost and Phelps[1]; those for $u \geq 36.0$ eV from scaling of P_c values[2] to connect onto Frost and Phelps' data.

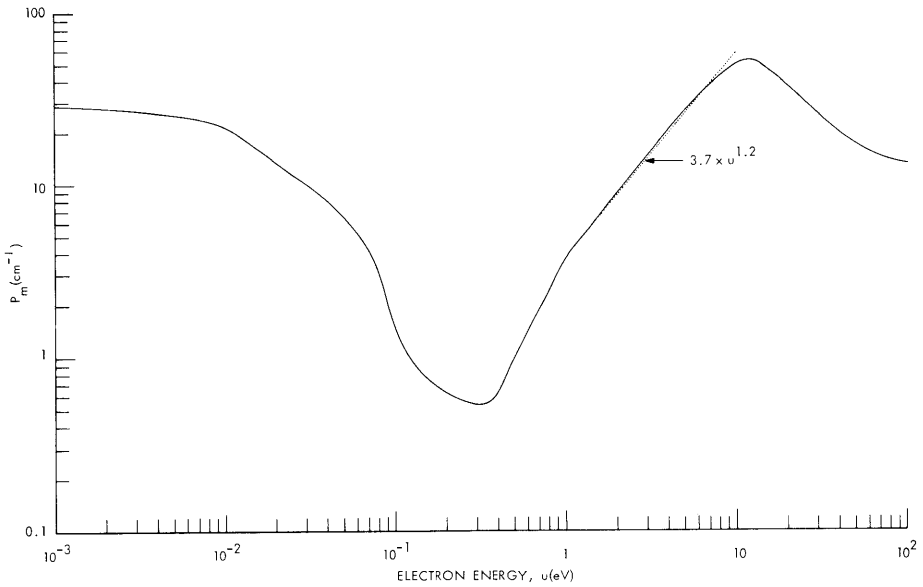

Fig. XI-1. Probability of collision for momentum transfer, P_m, as a function of electron energy, u. (Smooth curve drawn through unstarred values of Table XI-1.)

small effect on the results. The starred values of P_m in Table XI-1 are obtained from Fig. XI-1 by linear interpolation. These are added to improve the numerical integration.

The straight (dotted) line shown in Fig. XI-1 is given by

$$P_m \approx (3.7)u^{1.2}\ \text{cm}^{-1}. \tag{1}$$

This is a reasonably good approximation to the actual P_m in the energy range from ~1.0 to 10.0 eV.

For a spherically symmetric electron distribution function f_o (normalized to unity), the mobility is given[3] by

$$\mu = \frac{4\pi q}{3m} \int_0^\infty \frac{v^3}{\nu_m(v)} \frac{\partial f_o}{\partial v}\, dv, \tag{2}$$

where v is the particle speed, q and m are the electron charge and mass, respectively, and $\nu_m(v)$ is the collision frequency for momentum transfer at speed v. ν_m is given by $\nu_m(v) = p_o P_m(v)\, v$, where p_o is the "reduced pressure"[2] in Torr. The average collision frequency and mean-free path are given by

$$\nu_m = \int_0^\infty [p_o P_m(v)\, v] 4\pi v^2 f_o\, dv \tag{3}$$

and

$$\lambda = \int_0^\infty \left[\frac{1}{p_o P_m(v)}\right] 4\pi v^2 f_o \, dv. \tag{4}$$

For a Maxwellian distribution function with temperature V_e (eV), the expressions above can be rewritten

$$(\mu \cdot p_o)\left(\frac{cm^2 \cdot Torr}{V \cdot sec}\right) = \frac{(2.236\times10^7)}{V_e^{5/2}} \int_0^\infty \frac{u}{P_m(u)} e^{-u/V_e} \, du \tag{5}$$

$$(\nu_m/p_o)(sec^{-1} \cdot Torr^{-1}) = \frac{(6.709\times10^7)}{V_e^{3/2}} \int_0^\infty P_m(u)\, u\, e^{-u/V_e} \, du \tag{6}$$

$$(\lambda \cdot p_o)(cm \cdot Torr) = \frac{(1.128)}{V_e^{3/2}} \int_0^\infty \frac{u^{1/2}}{P_m(u)} e^{-u/V_e} \, du, \tag{7}$$

where u is electron energy in eV, P_m is in units of cm^{-1}, and $V_e = (kT_e/q)$, k being Boltzmann's constant, and T_e the electron temperature in °K.

The integrals in Eqs. 5, 6, and 7 have been computed numerically[4] for various values of V_e. The integrations were performed by using the trapezoidal rule, with the integrands evaluated at the electron energies listed in Table XI-1.[5] The results are shown in Figs. XI-2, XI-3, and XI-4 (curves 2a, 3a and 4a).

Also shown in Figs. XI-2, XI-3, and XI-4 (curves 2b, 3b, 4b) are values of μp_o, (ν_m/p_o), and λp_o calculated from Eq. 1, with $u = V_e$. That is, the relations $\mu = \frac{e}{m\nu_m}$, $\nu_m = p_o P_m(v)\, v$, and $\lambda = \frac{1}{p_o P_m(v)}$ have been evaluated at $v = \sqrt{\frac{2eV_e}{m}}$. This corresponds to a type of approximation frequently made. For the mobility (Fig. XI-2) the approximate values (curve 2b) are in good agreement with the results of the numerical integration (curve 2a). For the collision frequency and mean-free path, however, this is not the case. In general the approximate values of ν_m (curve 3b) are smaller than the computed values (curve 3a) by almost a factor of three, agreeing with the computed values only in the immediate vicinity of 7.3 Volts. The approximate values of λ (curve 4b) are all smaller than the computed values (curve 4a), with the ratio of the two varying from ~1.7 to ~3.4.

For some ranges of electron temperature the computed values of mobility,

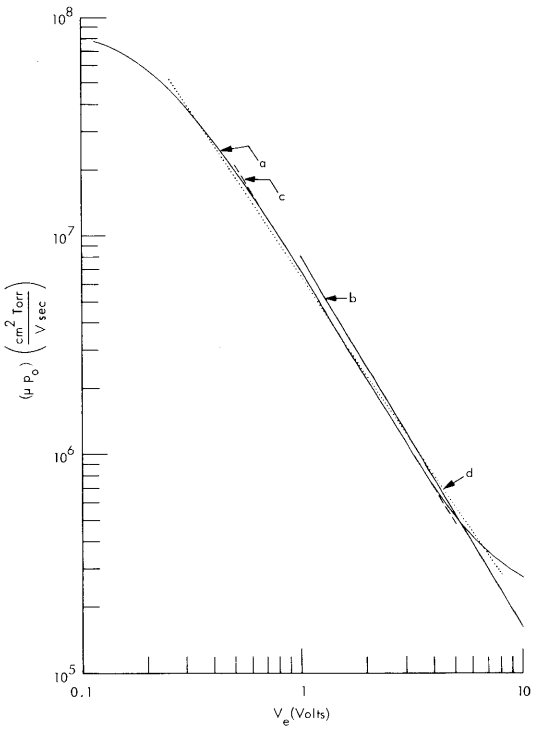

Fig. XI-2.

Mobility, μ, as a function of electron temperature, V_e, and reduced pressure, p_o.

Curve a: From numerical integration, Eq. 5.
Curve b: From approximation to P_m curve, Eq. 1.
Curve c: Approximation to result of numerical integration, Eq. 8.
Curve d: Simpler power-law approximation to result of numerical integration, Eq. 11.

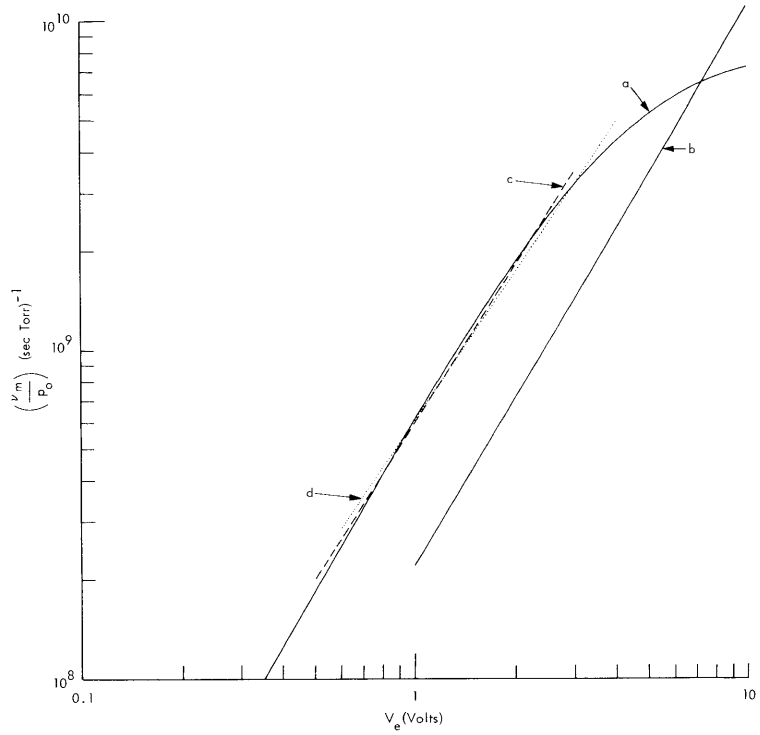

Fig. XI-3.

Collision frequency, ν_m, as a function of electron temperature, V_e, and reduced pressure, p_o.

Curve a: From numerical integration, Eq. 6.
Curve b: From approximation to P_m curve, Eq. 1.
Curve c: Approximation to result of numerical integration, Eq. 9.
Curve d: Simpler power-law approximation to result of numerical integration, Eq. 12.

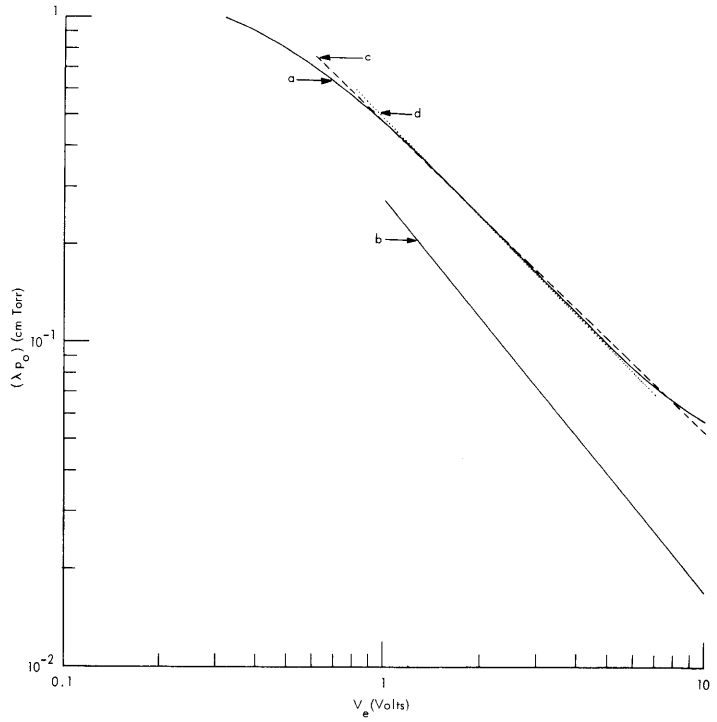

Fig. XI-4. Mean-free path, λ, as a function of electron temperature, V_e, and reduced pressure, p_o.

Curve a: From numerical integration, Eq. 7.
Curve b: From approximation to P_m curve, Eq. 1.
Curve c: Approximation to result of numerical integration, Eq. 10.
Curve d: Simpler power-law approximation to result of numerical integration, Eq. 13.

collision frequency, and mean-free path can be given by simple power-law relations with quite good accuracy. Examples of such relations, with approximate ranges of validity, are

$$\mu \cdot p_o \approx (6.86\times10^{6})\, V_e^{-1.64} \left(\frac{cm^2 \cdot Torr}{V \cdot sec}\right) \qquad 0.5 < V_e < 5.0\ V \tag{8}$$

$$\nu_m/p_o \approx (6.0\times10^{8})\, V_e^{1.61}\ (sec \cdot Torr)^{-1} \qquad 0.5 < V_e < 3.0\ V \tag{9}$$

$$\lambda \cdot p_o \approx (4.70\times10^{-1})\, V_e^{-0.95}\ (cm \cdot Torr) \qquad 0.6 < V_e < 10.0\ V \tag{10}$$

These relations are shown in Figs. XI-2, XI-3, and XI-4 as (dashed) curves 2c, 3c, and 4c. Less accurate, but somewhat more convenient for some purposes, are the approximate relations

$$\mu p_o \approx (6.43\times10^{6})\, V_e^{-3/2} \left(\frac{cm^2 \cdot Torr}{V \cdot sec}\right) \qquad 0.25 < V_e < 8.0\ V \tag{11}$$

$$\nu_m/p_o \approx (6.13\times10^{8})\, V_e^{3/2}\ (sec \cdot Torr)^{-1} \qquad 0.6 < V_e < 4.0\ V \tag{12}$$

$$\lambda p_o \approx (4.83\times10^{-1})\, V_e^{-1}\ (cm \cdot Torr) \qquad 0.8 < V_e < 7.0\ V, \tag{13}$$

which are shown in Figs. XI-2, XI-3, and XI-4 as (dotted) curves 2d, 3d, and 4d. Equations 8-13 are useful expressions for calculating the mobility, collision frequency for momentum transfer, and mean-free path for Maxwellized electrons in Argon.

G. L. Rogoff

References and Footnotes

1. L. S. Frost and A. V. Phelps, Westinghouse Research Laboratories Paper 64-928-113-P6, June 18, 1964. A graph of the momentum transfer cross section is also presented in L. S. Frost and A. V. Phelps, Phys. Rev. 136, A1538 (1964).
2. S. C. Brown, Basic Data of Plasma Physics, 1966 (The M.I.T. Press, Cambridge, Mass., 1967).
3. W. P. Allis, Electrons, Ions, and Waves (S. C. Brown, ed.) (The M.I.T. Press, Cambridge, Mass., 1967).
4. The computation was carried out on the IBM System 360 computer at the M.I.T. Computation Center.
5. For $V_e \geq 0.6$ eV all 50 unstarred values of P_m in Table XI-1 were used in the numerical integration. For $V_e < 0.6$ eV, however, because of computer limitations on the magnitude of the exponential in Eqs. 5-7, the 9 highest energy values of P_m were not used.

B. VELOCITY SPACE DIFFUSION IN A MAGNETIC FIELD

During the past quarter we have continued studies on the wave-particle interaction in the weak turbulence limit. It has been shown elsewhere[1] that to any order in perturbation theory the particles obey a diffusion equation. It has been found that stochastic particle acceleration and nonresonant mode coupling matrix elements are closely related. Essentially, by solving for either, one can find both.

We have recently extended these studies by considering the wave-particle interactions in a magnetic field. Basically, the same result emerges – that the distribution function to any order in perturbation theory obeys a diffusion equation. To order 2n, n waves diffuse particles along characteristics that are circles in $V_\perp V_\parallel$ space centered at $V_\parallel = \dfrac{\omega_1 \pm \ldots \pm \omega_n}{(k_1 \pm \ldots \pm k_n)_z}$.

Three specific nonlinear problems have been worked out by calculating velocity space diffusion constants to fourth order in perturbation theory. If electrostatic waves propagate almost parallel to the magnetic field at approximately half the electron cyclotron frequency, the particles can gain energy and the wave may be nonlinearly damped. This damping coefficient has been explicitly calculated.

We have applied the theory to particle acceleration by VLF turbulence ($\omega < \omega_{ce}$). Since low-frequency waves have low parallel phase velocities, they cannot effectively energize particles in the linear theory; however, in the nonlinear theory they can. Particle energization rates for a spectrum of whistler waves were estimated.

Finally, we discussed a nonlinear instability of a plasma confined in a mirror machine. In order to eliminate tremendous mathematical complication, we have considered only a rather extreme limit, $\frac{T_e}{T_i} \sim 10^{-3}$, and the density only slightly above stability threshold. We have shown, however, that in this case nonlinear growth rates may be significant, and it appears reasonable to speculate that they may be important for other more reasonable plasma parameters.

W. M. Manheimer

References

1. W. M. Manheimer and T. H. Dupree, "Weak Turbulence Theory of Particle Diffusion and the Nonlinear Landau Damping of Waves" (submitted to The Physics of Fluids).

C. NONLINEAR HARMONIC GENERATION AT PLASMA RESONANCES

The subject of this report is the generation of harmonics of an RF signal applied to a monopole probe immersed in the center of a low-density ($n \sim 10^8$ electrons/cm^3), low-pressure ($p \sim 0.4\ \mu$), DC discharge in Argon.

A simple theory considering the harmonics as generated by rectification in the nonlinear sheath, which is applicable to the sheath-plasma resonance, and some results for a dipole probe were discussed in a previous report.[1] It was shown that the voltage in the harmonic was proportional to the fundamental voltage to the power of the harmonic number.

A schematic diagram of the experimental apparatus is shown in Fig. XI-5. The data were taken by observing the harmonics reflected back from the exciting monopole (1" radius) and transmitted to a monopole receiver (3/32" radius) 4 inches from the exciter. The data were taken as follows: For fixed incident frequency f, the harmonic generation at 2f and 3f was observed as a function of discharge current.

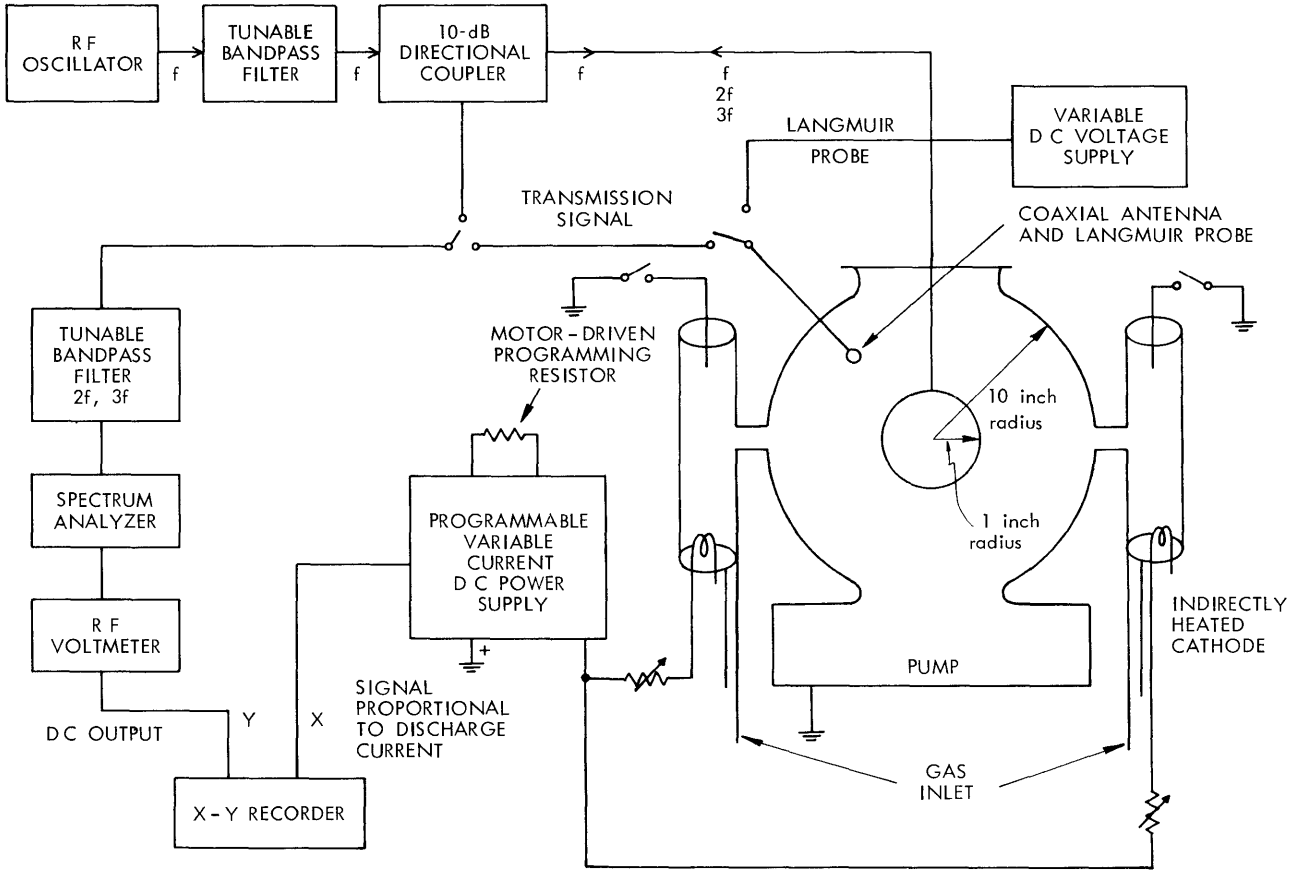

Fig. XI-5. Diagram of the experiment.

Then the incident frequency was varied and the measurements were repeated. Data runs were taken with the probe floating and biased slightly above and below floating potential.

The harmonic generation exhibited a more complex structure than the single peak observed for the dipole. Figure XI-6a exhibits the two main peaks, called types A and B, and the smaller low-current peak, called A^*. Biasing the monopole probe by a small amount (drawing less than 1 mA of current to it) shows that peaks A and A^* do not move and that peak B does move with bias. This is illustrated in Fig. XI-6b. Peak B is a manifestation of the sheath-plasma series resonance. The simple series circuit resonance frequency is $\omega_r = \frac{1}{\sqrt{LC}}$, where L is the plasma, and C is the sheath capacitance. Biasing the probe negatively will expand the sheath (that is, repel electrons); hence, C will decrease and ω_r will increase. The series resonance is a function of ω/ω_p, so, for fixed ω, the effect will show up as a decrease in ω_p for resonance. Biasing the probe positively will increase the resonant density. Again, see Fig. XI-6b.

Sketches of several different data runs are shown in Fig. XI-6. The low-current harmonic peak A^* is roughly 1/30 of the voltage of harmonic peak A, which is roughly 1/100 of the incident signal of 1 Volt. The third harmonic is seen to peak both at type A and type B resonances (Fig. XI-6f). The voltage for second and third harmonics exhibits the same dependence on fundamental voltage as for the dipole discussed above.

The type B peak in harmonic generation is due to the sheath-plasma resonance at the fundamental. This resonance at the fundamental can also be observed with an admittance meter (Fig. XI-6i). The locations of the A and A^* resonances are determined by a different mechanism. In Fig. XI-6a, peak A is a resonance at 150 MHz, and peak A^* is a resonance at 75 MHz. This can be understood by referring to Fig. XI-6c, in which the incident frequency has been doubled and the peaks have shifted to higher currents. An A^* peak now occurs at the same current that the A peak occurred at for 75 MHz. The only reasonable explanation is that a resonance occurs at 150 MHz for that current. If the A peak were a resonance at 75 MHz, then, for 150 MHz incident, a peak at 300 MHz would not be expected. If the B peak were a resonance at 150 MHz, then a peak in the harmonic generation of 150 MHz incident would also occur at the location of the B peak for 75 MHz incident.

It might have been argued that the type A resonance was a series resonance between the inductive plasma and the capacitive glass tube of 1/2 in. diameter surrounding the transmission feed line to the monopole. This was proved not to have been the case by using a much thinner transmission line sheathed by 1-mil teflon

with which any important capacitance would only be formed by the plasma. Types A and A^* peaks were observed to exist and to have the same properties as with the glass-sheathed transmission line. The only difference was that the type A peaks were smaller relative to type B for the teflon than for the glass.

This type A resonance is thought to be a plasma transmission resonance at the harmonic. If Fig. XI-6h is compared with Fig. XI-6a, peak A is seen to be enhanced relative to peak B in transmission. Considering Fig. XI-6g, a peak in transmission of the fundamental is also found near peak A. Messiaen and Vandeplas predict and have observed a transmission resonance for a dipole that does not move with bias.[2] Harmonic generation in the sheath, although not as strong as at peak B, also occurs at the location of peak A. It is this harmonic that is enhanced by plasma transmission resonance to yield the observed peak A. Both the theory of this mode and its ability to generate harmonics itself, that is, the A^* peak, will be worked out in the future.

If the current at which the peak occurs is plotted as a function of incident frequency, it is found that the peak current varies approximately as the square of the incident frequency for peaks A and A^*, and as the fourth power of the frequency for peak B. If the assumption is made that electron density n is proportional to discharge current I, then for peaks A and A^*, $f \sim n^{1/2}$, and for peak B, $f \sim n^{1/4}$. A plasma effect independent of the sheath surrounding the antenna would not move with bias and should have a resonant frequency proportional to the plasma frequency, and hence proportional to $n^{1/2}$. The simple expression for the monopole sheath-plasma resonance is $f_r = \sqrt{\frac{s}{a+s}}\, f_p$, where a is the probe radius, and s is the sheath size taken as 5 Debye lengths.[3] For the experimental parameters considered, s is approximately 0.5 cm, and a is 2.54 cm, so $f_r \sim \sqrt{s}\ f_p$. Since the Debye length $\lambda_D \sim \sqrt{\frac{T}{n}}$ and the plasma frequency $f_p \sim \sqrt{n}$, then $f_r \sim (Tn)^{1/4} \sim n^{1/4}$ if the temperature T is constant.

In reality, the average variation found for types A and A^* was $f_A \sim I^{1/2.34}$ with little scatter in the data, and $f_B \sim I^{1/3.61}$ for type B peaks with somewhat larger scatter in the exponent from run to run.

$I = nev_dA$, where n is the electron density, e is the electronic charge, v_d is the electron drift velocity, and A is an area normal to the flow. v_d is proportional to the square root of the discharge voltage for high E/p discharges (E/p ~ 1000 Volts/cm-Torr). The voltage across the discharge only increases approximately 10 per cent for an increase of a factor of 10 in the current. This small variation in the drift velocity with current pushes the type A peaks in the desired direction, but pushes the type B peaks in the wrong direction. Langmuir probe studies yield an electron temperature increasing from 9 to 10 eV for the increase

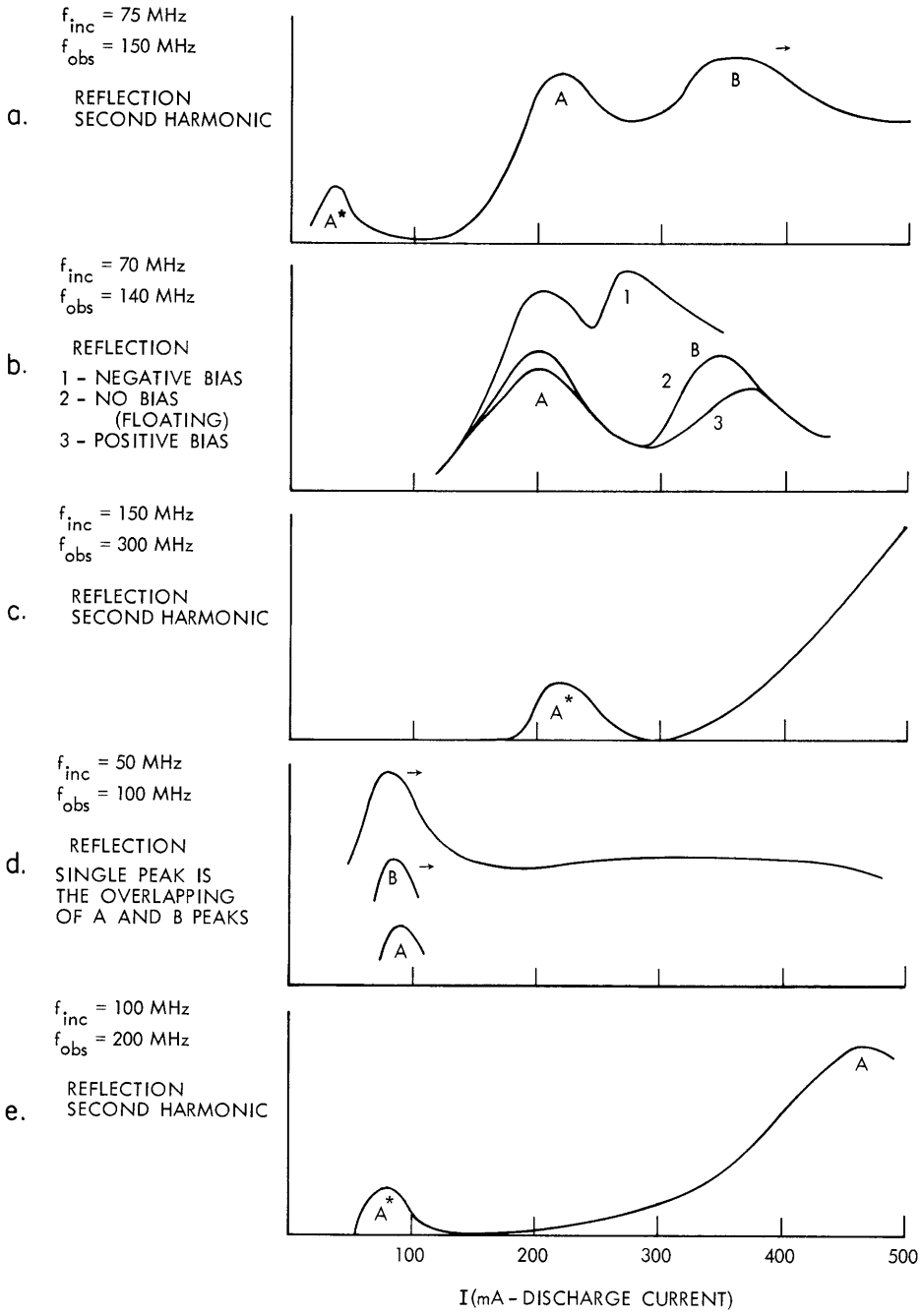

Fig. XI-6. (a-e) Typical experimental data.

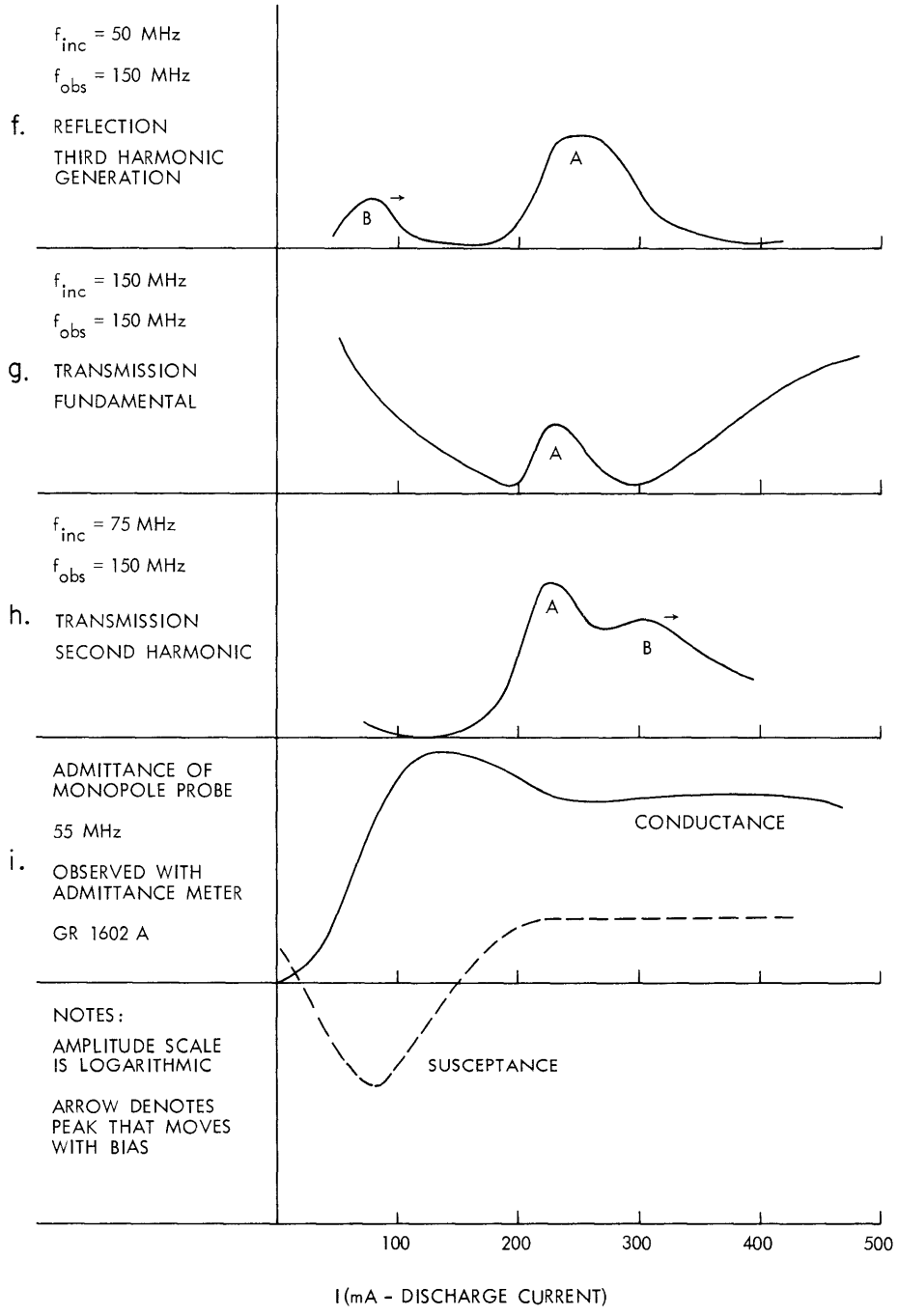

Fig. XI-6. (f-i) Typical experimental data.

of a factor of 10 in current. This increase will push the type B peaks toward the A peaks (the desired direction).

Coupling between the resonances cannot explain the pulling together of peaks A and B because when peak A^* is excited, there is no large peak nearby to pull it, and yet it also has an $I^{1/2.33}$ dependence similar to peak A. Stern has found that coupled resonances in his plasma moved as a function of incident power.[4] As the incident power level is increased in this experiment, these peaks do not change location.

The differences in the slopes from those expected may also be due to the fact that the complete theory for the geometrical resonance[5] has not been used, and the theory for the type A peak has not yet been developed in detail. Also, this complex discharge is not fully understood. The slopes are close enough to those expected, however, to make the difference not too important.

A. J. Cohen

References

1. A. J. Cohen, Quarterly Progress Report No. 85, Research Laboratory of Electronics, M.I.T., April 15, 1967, p. 103.
2. A. M. Messiaen and P. E. Vandenplas, Electronics Letters, Vol. 3, No. 1, January 1967. They can predict theoretically the occurrence of, but cannot account for, the experimental location of the transmission resonance of a dipole immersed in a sphere of plasma.
3. R. S. Harp and F. W. Crawford, J. Appl. Phys. 35, 3436 (1964).
4. R. A. Stern, Appl. Phys. Letters 4, 80 (1964).
5. R. Buckley, Proc. Roy. Soc. (London) A290, 186 (1966); J. Plasma Phys. 1, (2), 171 (1967).